Informatics in Medicine Unlocked 26 (2021) 100736

Contents lists available at ScienceDirect

Informatics in Medicine Unlocked

journal homepage: www.elsevier.com/locate/imu

Automated detection of hypertension using wavelet transform and nonlinear techniques with ballistocardiogram signals

Jaypal Singh Rajput [a], Manish Sharma [a,*], Divyash Kumbhani [a], U. Rajendra Acharya [b,c,d]

[a] Department of Electrical and Computer Science Engineering, Institute of Infrastructure Technology Research and Management, Ahmedabad, 380026, India
[b] Department of Electronics and Computer Engineering, Ngee Ann Polytechnic, Singapore, Singapore
[c] Department of Bioinformatics and Medical Engineering, Asia University, Taichung, Taiwan
[d] Department of Biomedical Engineering, School of Science and Technology, SUSS, Singapore

ARTICLE INFO

Keywords:
Hypertension
BCG signal
Supervised machine learning
Hypertension BCG signal classification
Empirical mode decomposition
Wavelet decomposition (DB8)
Signal fractal dimension
Log Energy
Shannon entropy

ABSTRACT

Arterial hypertension (HT) is a common cardiovascular disease and, if not treated at an early stage, can lead to serious complications. It is difficult to precisely describe because it is a dynamic physiological state. Monitoring of HT is subjective and prone to mistakes. Therefore, various computer-assisted diagnostic methods have been designed. The proposed work is based on ballistocardiography (BCG) signals for the diagnosis of healthy control (HC) and HT subjects. The identification of HT based on BCG signals of 30-s duration using empirical mode decomposition (EMD) and wavelet transform (WT) with nonlinear techniques is proposed in this work. The BCG signal is decomposed into five sub-bands (SBs) using WT and five-level of intrinsic mode functions (IMFs) using EMD. Then, the various non-linear features are calculated for all five-level wavelet decomposition and IMFs. The non-linear features are extracted from the SBs of WT and IMFs of EMD. These features are fed to ensemble gentleboost (EGB) classifier with 10-fold cross-validation strategy for automated detection of HC and HT groups. In this study, the performance of WT and EMD techniques are compared. The proposed HT identification model accomplished the highest average classification accuracy of 89% using WT method. In future, we plan to extend this work using more BCG data.

1. Introduction

The systolic blood pressure (SBP) more than or equal to 140 mmHg, or diastolic blood pressure (DBP) more than or equal to 90 mmHg, is considered as hypertension (HT) [1,2]. Classification of hypertension in to several groups is shown in Table 1 [1]. HT increases the force exerted by blood against the walls of arteries that transport oxygen-rich blood from the heart to the rest of the body [2–4].

Risky cardiovascular diseases are on the rise and HT has become more prevalent. HT is usually diagnosed through a prolonged period of elevated arterial blood pressure. A recent report from the World Health Organization (WHO) suggests that more than 40% of adults (aged 25 and over) are affected by HT; thereby signifying that globally, more than 1 billion people would suffer from the related diseases [5,6]. HT causes serious complications such as stroke, heart attack, kidney failure and many more in the absence of proper treatment [5]. Consequently, the recent WHO report states that HT leads to 9.4 million deaths annually [5,6]. Many people not even realize that, they are suffering from the silent disease (HT). Therefore, it is crucial to detect HT in the early stage to ease the problem and avoid further complications [5,6].

The traditional method to measure blood pressure is the cuff based mercury sphygmomanometer [6]. The drawback of this method is the need for specialists to obtain the accurate readings. It is also uncomfortable and unsuitable for usage in a home environment [5]. Moreover, HT is a complex condition, may lead to unpredictable fluctuations in blood pressure of an individual [5]. Analyzing the disease status via sphygmomanometer measurements may not be accurate, since the instrument only provides discrete results [5]. Therefore, novel method which can overcome the above problems is needed.

One such novel method is the ballistocardiography (BCG), which is a noninvasive technique. BCG analyzes the heartbeat induced repeated motions of the human body and creates a graphical representation of the same [6].

Generation of BCG signal- Rapid acceleration of the blood during its movement in the blood vessels of the body from the diastolic and systolic periods gives rise to the repeated motions [5,7]. BCG picks these repeated motions, analyzes it and provides information about the mass of circulating blood and heart during the cardiac cycle [6]. In the atrial systolic cycle, when blood is pumped into the blood vessels,

* Corresponding author.
E-mail address: manishsharma.iitb@gmail.com (M. Sharma).

https://doi.org/10.1016/j.imu.2021.100736
Received 1 July 2021; Received in revised form 22 August 2021; Accepted 14 September 2021
Available online 20 September 2021

Table 1
Hypertension classification based on blood pressure readings taken in the clinic [1].

Classification	SBP	DBP
Healthy BP	<130	<85
Pre-HT BP	130–139	85–89
Stage 1 HT BP	140–149	90–99
Stage 2 HT BP	≥160	≥100

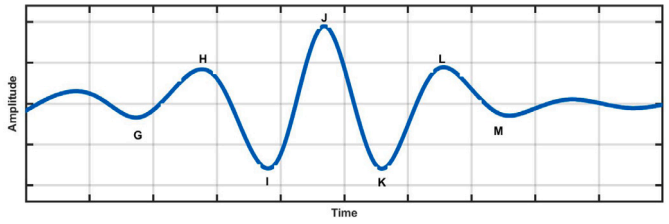

Fig. 1. BCG signal generated from database.

the body's center of mass moves towards the head [7]. Conversely, as the blood moves away from the heart and towards the peripheral vessels, the center of mass moves towards the feet [7]. Cardiac activity, respiration, body movements all contribute to this shifting of center of mass, which then generates the BCG waveform, analyzed as blood distribution changes during the cardiac cycle [7].

It is possible to embed BCG sensors in households without the need for specialized personnel. As a result, it would have a positive impact on the current e-health systems [7]. This would also reduce a patient's stress and emotion levels during checkups and increase their attention responses. Fig. 1 represents the typical example of a BCG signal with the letters designating the waves [5,7]. However, Fig. 1 represents the relationship between blood pressure and systolic and diastolic cycles of the heart [5,7].

In Fig. 1, the waveforms starting from G wave till K wave represent the systolic cycle of the heart and it is same as QRS wave in ECG signal. The diastolic cycle's blood pressure is represented by the proceeding K wave till the end of M wave. Hence, using systole (G to K wave) and diastole cycle (K wave to end of M wave), we can measure the heart rate, heart rate variability, body movement, and respiratory system of patients using BCG signal. These waves are present in the normal BCG signal [5,7].

Related works done on HT and BP detection using BCG signal: Y. Song et al. [8] used heart rate variability (HRV) signal to identify hypertension and health control BCG signals. The maximum classification accuracy of 74.5% is obtained with Naive Bayes classifier using non-linear features. Similarly, Liu et al. [5] extracted HRV signals from BCG signal and yielded maximum classification accuracy of 84.5% in detecting HT and normal BCG signals.

Chen et al. [9] obtained SBP and DBP from the BCG and PPG signal using linear regression technique. Authors reported an error (9 ± -5 of mean and standard deviation) for SBP and 1.8 ± -1.3 for DBP. Lee et al. [10] diagnosed the SBP and DBP from BCG signal using ANN. The mean and standard deviation errors obtained for SBP and DBP are 0.0123 ± 6.7542, and 0.0532 ± 5.8317, respectively. In another study Seok et al. [11] used CNN for the diagnosis of SBP and DBP using BCG signals. The two channel BCG signal have been recorded at the resting state and during exercise. In the resting state, SBP and DBP errors are 0.93 ± 6.24, and 0.21 ± 5.42, respectively. On the other hand, the SBP and DBP errors for exercise session are -1.12 ± 8.74, and -0.728 ± 4.87, respectively. Hence, very few works have been done on detecting HT using BCG signals.

Although electrocardiography (ECG) and photoplethysmography (PPG), BCG is a non-contact approach which does not require skin contact [9–11]. In addition to this BCG can capture information about heartbeats without bothering patients and is ideal for long-term assessment and monitoring [9–12]. However, the BCG-based pulse transient time (PTT) is significantly correlated with blood pressure [9–11]. Additionally, if the signal quality declines, peak value of PPG or ECG cannot be identified, which may reduce the classification accuracy.

Table 2
Details of BCG database used in this study.

Parameter	HT subjects	HC subject
Number of subjects	61	67
Gender (Female/Male)	38/33	32/35
Age in years	55.630 ± 7.930	53.265 ± 9.198
HR	77.132 ± 9.210	73.602 ± 8.301
BMI	24.303 ± 3.599	23.699 ± 3.301
SBP	155.612 ± 11.199	112.101 ± 15.699
DBP	103.631 ± 11.210	74.432 ± 6.321

HR = Heart Rate, BMI = Body Mass Index, SBP = Systolic Blood Pressure(mmHg), SBP = Di-systolic Blood Pressure (mmHg).

The limitation of the BCG signals are as follows. The definition of BCG signal in the literature is still not clear [7,12]. The physiological significance of BCG displacements and its clinical significance are not annotated yet. The signal quality gets affected during breathing, posture, and sensor adherence [7,12]. Signals from healthy and diseased subjects, as well as a variety of body types/sizes and ages, can be obtained for analysis [7,12].

The proposed HT identification model accomplished the highest average classification accuracy of 89% using WT method. In this study, we proposed an automated diagnosis of HT using BCG signals. We did not extract HRV from BCG signal as authors did in the literature [5]. We reported high detection accuracy and features extraction from BCG signals is fast as requires less computation time. To the best of our knowledge, we are the first group to develop the automated system to detect HT using BCG signals.

In this study, we have decomposed the BCG signal into five sub-bands (SBs) using wavelet transform and five IMFs with EMD method. A non-linear SFD, SHN, and LE features are extracted from all IMFs and wavelet SBs. All extracted features are fed to various classifiers for automated detection of HT class.

Using conventional approaches, well-trained and skilled humans may be able to identify HT-associated complications using BCG signals, but may find it difficult to infer information about BP measurement from visual analysis of BCG signals. Using an automated CAD system, it is possible to diagnose HT from BCG signals accurately, rapidly, and with little pre-processing.

Rest of the paper is organized as follows: Section 2 described the database used in this study. Section 3 explained the methods used, followed by results in Section 4. Section 5 discussed in detail the results obtained and summary of the paper is given in Section 6.

2. Database

The BCG signal was recorded for the entire night when subjects were sleeping. A total of 128 BCG signals have been recorded [5]. The sampling frequency of the BCG signal is 100 Hz. In this work, we have used BCG signals from 67 HC and 61 HT subjects [5]. The lengthy (13 h) BCG signals were segmented into 30 s epochs. Hence, we obtained 61525 and 71413 BCG epochs of HT and HC subjects, respectively. Hence, we have a total of 132938 BCG signal epochs. Figs. 2–3 shows the sample HC and HT BCG signals obtained from the database, respectively. Similarly, Table 2 represents the details of BCG database used in this study. The BCG database can be accessed from this link: https://doi.org/10.6084/m9.figshare.7594433.v2.

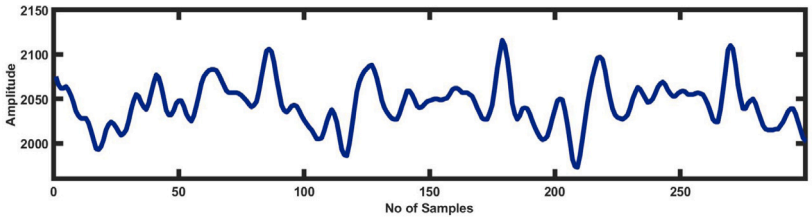

Fig. 2. Typical normal BCG signal.

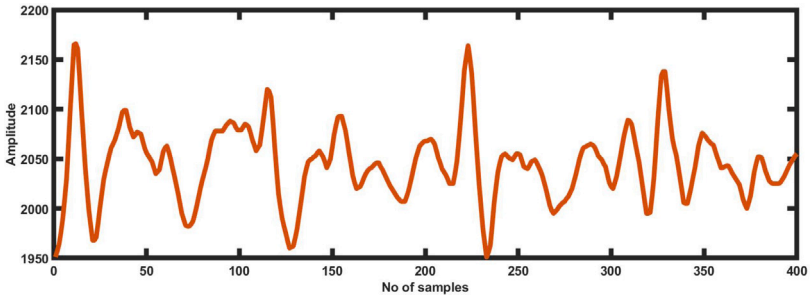

Fig. 3. Typical HT BCG signal.

3. Methodology

The flow of methodology employed in this study is shown in Fig. 4. The BCG signals are downloaded from the public database. Then BCG signals are segmented into the 30 s of epochs. Hence, we have obtained 132938 BCG signal epochs. In addition to this, we implemented WT and EMD on these segmented BCG signal epochs. Then the BCG signals are decomposed in to five-levels by WT (DB8) method. Hence, we have obtained six sub-bands from each 30 s BCG epochs. Similarly, on the other hand, each BCG signal epochs are decomposed into the five-intrinsic mode function (IMF) using EMD method. Various features (SFD, SHN, and LE) are extracted from the sub-bands and IMF of each BCG signal. The SFD, SHN, LE features computed from various sub-bands and IMF are applied to the various machine learning classifiers. Proposed block diagram of automated detection of HT using BCG signals is shown in Fig. 4.

3.1. Pre-processing of BCG signal

3.1.1. Segmentation

To increase the computation speed and performance of the classifier 13hr BCG signal recording are segmented into the 30 s signals.

3.1.2. Z-score normalization

Z-score normalization was used to eliminate the problem of amplitude scaling [4,13,14]. Each BCG signal's mean and standard deviation were calculated. The z-score can be computed using below mentioned formula:

$$Z = \frac{X - K}{\sigma}$$

where X is the values of the BCG signal to be normalized. K is the mean of BCG signal, and σ is a standard deviation of BCG signals.

3.2. Wavelet transform method

The BCG signal epochs are decomposed in to six SBs (five-level) using the Daubechies wavelet (DB8) mother wavelet function [15–19].

Out of six sub-bands, five SBs (SB2-SB6) are detailed and one (SB1) is approximated as shown in Fig. 5. Additionally, the frequency components having an important characteristic can be withheld using the five-level decomposition. Hence, we have chosen five-level wavelet decomposition. Fig. 5 depicts the original BCG signal (top) epoch and its wavelet decomposition for normal (HC) and hypertension (HT) class.

3.3. Empirical mode decomposition method (EMD)

It is a simple, direct, versatile, and data-dependent nonlinear analysis tool used widely for the classification of physiological signals [3,20]. The IMF decomposed large amounts of complex data into a manageable number of IMFs, based on the local time and scale characteristics of the data. Hence, for decomposition, every IMF meets two basic key criteria: (1) The total number of extrema and zero crossings in the entire data segment must be identical or differ by no more than one. (2) The envelope defined by the local maxima and minima must have a mean value of zero. The more details of EMD decomposition of data into IMF are described in [20]. In the proposed study we have produced IMF-1 to IMF-5 for the HT and HC classes using EMD method as shown in Fig. 6. We have obtained optimum and highest results using IMF1-IMF5 levels.

3.4. Features used

In supervised machine learning, optimum feature selection is based on trial and error methods. Similarly, we have obtained the optimum features are Shannon entropy (SHE) [21], signal fractal dimension (SFD) [22,23] , and log energy (LE) [16,24,25] for the classification of HC and HT BCG signal after the trial of n number of features. All three features were computed from each sub-bands (SBs) produced by WT and IMFs of EMD methods.

3.4.1. Shannon entropy (SHN)

It is a measurement of disorder, uncertainty, or unpredictability in a given set of BCG signal epochs [26–31]. To discriminate HC and HT classes SEN is found to be very effective. The SHN can be defined as :

$$SHN = -\sum_{i<0} x_i log_2(x_i) \quad (1)$$

The ith sample of the wavelet coefficient sequence $x(n)$ of length N is represented by x_i.

3.4.2. Log Energy (LE)

Log energy of a signal is computed by evaluating the logarithm of energy of the BCG signal [22,24]. It is defined as [16,24,25,32]

$$LE_{le} = \sum_{n \epsilon Z} \ln(|x(n)|)^2 \quad (2)$$

In Eq. (2), LE_{le} is LE with respect to sub-band, and $x(n)$ is the wavelet time series corresponding to sub-band n, for $n \in 1, 2, 3, 4, 5, 6$.

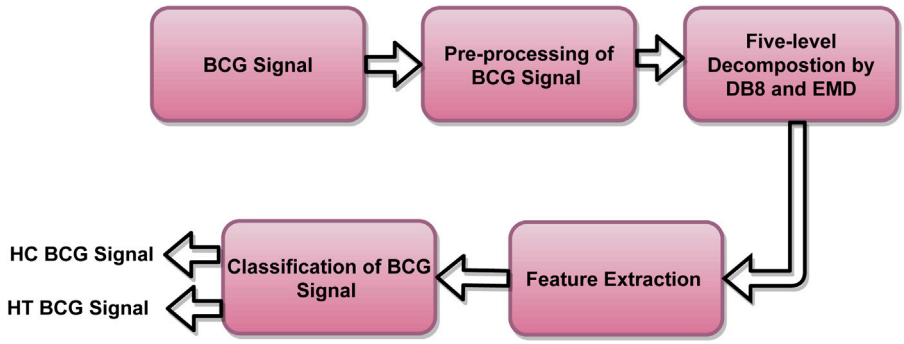

Fig. 4. Proposed block diagram of automated detection of HT using BCG signals.

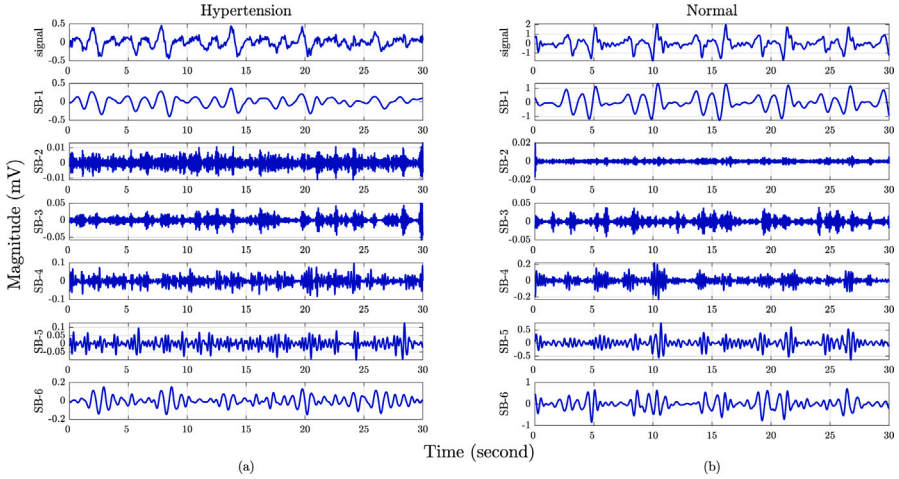

Fig. 5. Different sub-bands obtained using wavelet transform with BCG signals. SB2-SB6: detailed and SB1: approximate sub-band. (a) HT, and (b) Normal subject.

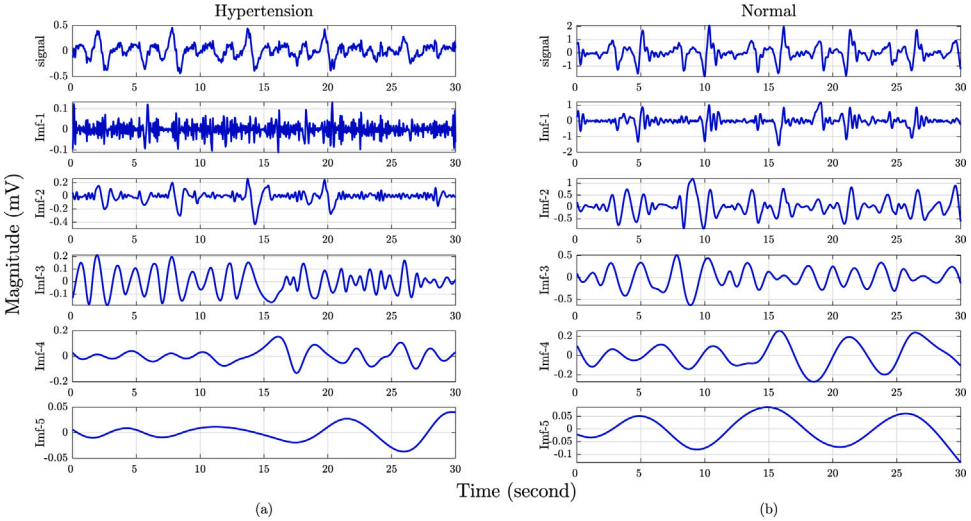

Fig. 6. Five levels of IMFs obtained using EMD with BCG signals: (a) HT, and (b) Normal subject.

3.4.3. Signal Fractal Dimension (SFD)

It is mostly used to compare the similarity and complexity of BCG epochs [22,23,33]. Mathematical representation of SFD is given below:

$$SFD = \frac{log(P_j)}{log(\frac{1}{j})} \quad (3)$$

In Eq. (3), the number of fractals/patterns are represented by P_j. The inverse of the factor that was used to break down the object into P_j is j.

The extracted features (SHN, SFD, and LE) are arranged to form a feature matrix. Finally resulting feature matrix is labeled (0 for HC and 1 for HT class) and supplied into the classification process to classify HC and HT BCG signals.

Table 3
Summary of results obtained for WT and EMD methods.

Parameter	WT %	EMD%	Classifier
Accuracy	89	78.7	
Sensitivity	86.95	77	
Specificity	90.84	80.16	EGB
F1-score	88.28	77	
Precision	89.66	76.97	

Table 4
Confusion matrix obtained for WT method using EGB classifier.

	HT	HC
HT	55161	6364
HC	8276	63137

Table 5
Confusion matrix obtained for EMD method using EBT classifier.

	HT	HC
HT	47351	14171
HC	14140	57265

3.5. Performance parameters of classifiers used

In the proposed study, we have used the ensemble gentleboost (EGB), ensemble bagged tree (EBT), support vector machine (SVM), K-nearest neighbor (KNN), and tree (TR) classifiers. However, the best classification accuracy is obtained using ensemble GentleBoost classifier. The optimum classification accuracy of 89% was obtained in the proposed work, using a 10-fold cross-validation approach. The following parameters are considered while training the EGB classifier: Learners = 71, Splits = 131255, Learning rate = 0.2745.

3.6. Ensemble GentleBoost classifier

It has been utilized in computer vision and machine learning, where it outperformed conventional target detection methods, detection and prediction of audio, video, images, and 1D signal results [34]. It uses a quadratic objective function of margin, which increases more slowly than the exponential function of margin used by AdaBoost, to give less weight to misclassified samples [35]. Importantly, GentleBoost is a method used to reduce exponential loss that uses decision trees as base learners. However, it is found to have a lower ensemble error than the other ensemble techniques [36].

Table 8
Summary of highest accuracy obtained using various classifier.

S no.	EMD (accuracy %)	WT (accuracy %)	Classifier
1	78.70	89	EGB
2	76.70	87.1	EBT
3	72.39	86.77	KNN
4	71.31	84.35	SVM
5	68.33	73.11	TR

Table 9
Comparisons of highest accuracy obtained using various classifiers and methods.

S no.	EMD (Acc%)	WT (Acc%)	(Acc%)	Classifier
1	78.70	89	–	EGB
2	–	–	56	ANN
3	63.6	69.79	–	LSSVM
4	71.31	84.35	–	SVM

4. Results

The proposed work classified HT and HC BCG signals using WT and EMD decomposition methods. SFD, LE, and SHN features yielded the optimum performance with the EGB classifier. A total of 132938 BCG signal epochs were obtained from 128 BCG signals. Out of which 61525 are from HT and 71413 belonged to the HC BCG signal class.

Experimental work has been computed on a personal computer using MATLAB 2016b software licensed version (9.10). In addition to this, the hardware configuration of a personal computer is as follows: RAM (16GB), HDD (1TB), Processor (Intel Xenon *i*7), Graphics card (4GB).

It can be noted Table 3, that the WT method obtained the highest classification accuracy of 89%, while EMD obtained 78.7% using an EGB classifier.

Tables 4–7 represents the individual confusion matrix for HC and HT classes, as well as performance parameters obtained using WT and EMD methods with 10-fold CV approach.

The highest performance obtained by other classifiers SVM, KNN, TR, and EBT classifier are mentioned in Table 8.

Table 6
Performance of various features obtained for EMD method using EGB classifier.

Feature	Class	Acc %	Pre %	Sen %	Spe%	F1%	Overall Acc %	kappa	Training Time	Prediction speed
SFD	HT	60.96	61.7	60.96	67.41	61.33	64.4	0.284	1118.2 s	11000 obs/s
	HC	67.46	66.71	67.41	60.96	67.05				
SHN	HT	61.74	64.94	61.74	71.28	63.3	66.9	0.331	1053 s	10000 obs/s
	HC	71.25	68.38	71.28	61.74	69.8				
LE	HT	62.93	65.89	62.93	71.94	64.38	67.8	0.35	921.61 s	11000 obs/s
	HC	71.94	69.25	71.94	62.93	70.57				
SFD+SHN+LE	HC	**76.97**	**86.95**	**89.66**	**88.41**	**88.28**	**78.7**	0.57	1278.5 s	17000 obs/s
	HT	**80.23**	**90.84**	**88.41**	**89.66**	**89.61**				

Table 7
Performance of various features obtained for WT method using EGB classifier.

Feature	Class	Acc %	Pre %	Sen %	Spe%	F1%	Overall Acc %	kappa	Training Time	Prediction speed
SFD	HT	68.56	69.9	68.56	74.56	69.22	71.8	0.432	879.48 s	12000 obs/s
	HC	74.56	73.35	74.56	68.56	73.95				
SHN	HT	77.86	79.62	77.78	82.85	78.69	80.5	0.607	1738.9 s	11000 obs/s
	HC	82.65	81.23	82.85	77.78	82.03				
LE	HT	82	80.34	82	82.72	81.16	82.4	0.646	865.85 s	14000 obs/s
	HC	82.72	84.21	82.72	82	83.46				
SFD+SHN+LE	HC	**89.66**	**86.95**	**89.66**	**88.41**	**88.28**	**89**	**0.78**	**1549.38 s**	**20000 obs/s**
	HT	**88.41**	**90.84**	**88.41**	**89.66**	**89.61**				

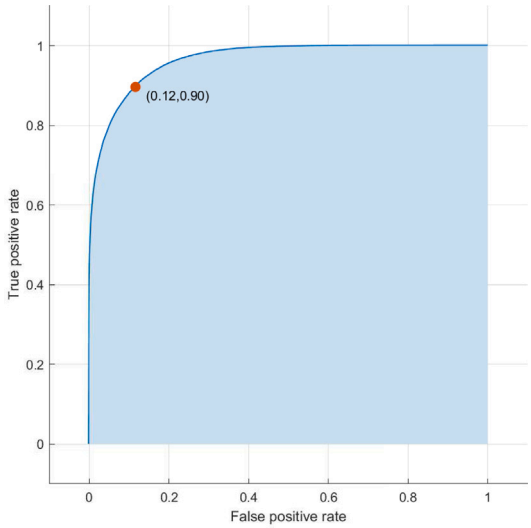

Fig. 7. Receiver operating characteristics obtained for WT method using EGB classifier.

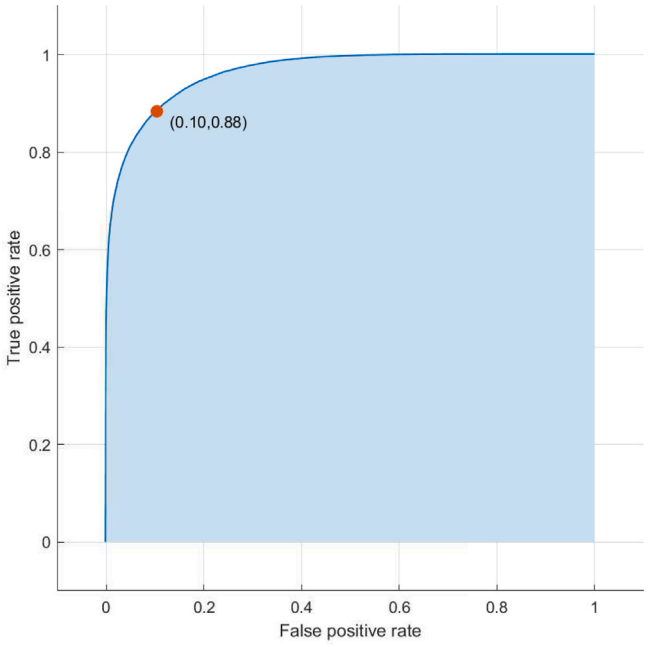

Fig. 8. Receiver operating characteristics obtained for EMD method using EGB classifier.

Table 9 compares the classification performance obtained using EGB, SVM, least-square support vector machine (LSSVM), and artificial neural network (ANN) classifiers.

Additionally, mean and standard deviation of SFD, SHN, and LE features obtained using WT and EMD methods are mentioned in the Tables 10–12.

The highest AUC = 0.96 and 0.88 obtained by WT and EMD methods are shown in the Figs. 7–8, respectively.

5. Discussion

In this study, we have used the open-source database of BCG signals consisting of 61 HT and 67 HC subjects with approximately 13 h of recording. Further, to reduce the computation time, the database is segmented in to epochs of 30 s. Following segmentation, we have obtained 71413 epochs of HC and 61525 epochs of HT. The proposed work has used direct BCG signal and decomposed it in to six SBs (five-level) using WT, and five-IMFs using EMD method.

This work is carried out using MATLAB software. However, the prediction speed and training time of the EMD method taken is 1700 obs/sec, 1278 s, respectively. Similarly, the WT method has taken 1549 s for training time and 2000 obs/sec for prediction speed. Importantly, the proposed work is based on a diagnosis of HT and HC BCG signals using WT and EMD methods. The WT (five-level) method yielded the highest classification accuracy of 89%, the sensitivity of 86.95%, specificity of 90.84%, and precision of 89.66%, respectively. Similarly, the EMD (five-level-IMF) method obtained the classification accuracy of 78.7%, the sensitivity of 77%, specificity of 80.66%, and precision of 76.97%, respectively. In addition to this, both methods (WT and EMD), have the same level of decomposition, and same features are extracted (SFD, SHN, and LE). Hence, the wavelet-based method obtained the highest performance as compared to the EMD.

The Table 10 representing the SB5 of WT method have a larger difference between HC and HT classes, while SB1 has obtained smaller differences in terms of mean and standard deviation values obtained from SFD feature computation. Similarly, IMF1 of EMD decomposition have the larger difference, while IMF5 have smaller differences. On the other hand, Tables 11 and 12 represents the distinct difference (WT and EMD method) among the SBs and IMFs of HC and HT classes of BCG signals using LE and SHN features. The classification results are higher as compare to the SFD feature as shown in the Tables 6–7. Hence, the combined classification results obtained from SFD, SHN, and LE features are optimum and highest as compare to the other non-linear features. However, it can be noted from Table 8 that, an EGB classifier yielded highest classification accuracy of 89% (using WT) and 78.70% (using EMD). Figs. 7–8 representing the area under the curve (AUC) of 0.96 and 0.88 for WT and EMD methods, respectively.

The performance comparison using LSSVM, SVM, ANN, and EGB classifiers is shown in Table 9. ANN obtained the highest classification accuracy of 56%. On the other hand, the classification speed of LSSVM classifier is slow and the highest accuracy of 69.79% is obtained. However, SVM classifier obtained a classification accuracy of 84.35% using WT method. The classification accuracy of 89% is obtained using EGB classifier which is the highest for this study.

It can be noted from Table 13 that Liu et al. [5] used HRV signal extracted from BCG signal to classify HC and HT class. Authors obtained the accuracy of 84.45% using various linear, non-linear, time domain, and frequency domain features. They proposed the class association rule (CAR) method, which provided the physiological status of the patients. The CAR method combined different classifiers using some specific rules as designed by authors for the classification of HT and HC BCG signals. They have used large number of features, but we have used fewer number of features and obtained a classification accuracy of 89% using the same database.

Y. song et al. [8] applied ensemble empirical mode decomposition (EEMD) method on HRV signal for the classification of cardiovascular disease. The authors extracted various linear, non-linear, time, and frequency domain features from HRV signals and classified them using Naive Bayes classifier. They obtained 74.35% classification accuracy using various non-linear features. However, the authors used a small and balanced database. On the other hand, in this study, we have used few nonlinear features and obtained higher classification accuracy using EGB classifier.

The advantages of the proposed work are given below:

The proposed method has obtained the optimum performance (89% accuracy) using the WT method. In the literature, this may be the first paper to detect HT from BCG signals using WT and non-linear features. For this purpose, we have used a 30-sec epoch of BCG signal. As a result, our method is faster and does not require expensive pre-processing techniques. Correspondingly, the HT may be diagnosed from BCG signal-based systems, that are non-invasive, robust, and accurate without direct BP measurement. The developed system is

Table 10
Statistical parameters (mean (M) and standard deviation (STD)) calculated for SFD feature obtained from EMD and WT methods.

		WT - 5 level				EMD - IMF - 5			
		HT		HC		HT		HC	
		M	STD	M	STD	M	STD	M	STD
SFD	SB1	1.0131	0.0025	1.0134	0.0025	1.4513	0.1387	1.3792	0.1681
	SB2	2.0846	0.0283	2.0788	0.0281	1.0881	0.0439	1.0753	0.0526
	SB3	1.909	0.0073	1.9074	0.0075	1.0132	0.0057	1.0121	0.0078
	SB4	1.5582	0.0661	1.5694	0.0671	1.003	0.0019	1.0028	0.0022
	SB5	1.2184	0.0335	1.1968	0.0363	1.0011	0.0015	1.0011	0.0015
	SB6	1.0422	0.0079	1.0446	0.0084				

Table 11
Statistical parameters (mean (M) and standard deviation (STD)) calculated for SHN feature obtained from EMD and WT methods.

		WT - 5 level				EMD - IMF - 5			
		HT		HC		HT		HC	
		M	STD	M	STD	M	STD	M	STD
SHN	SB1	2778.067	15195.27	2379.743	11468.18	2810.161	20096.44	2568.514	17575.08
	SB2	−0.5682	2.3777	−0.6773	4.3088	3223.753	21439.51	2532.915	14844.57
	SB3	−1.1165	29.6834	0.4277	134.273	375.678	3330.576	287.9045	2807.771
	SB4	16.0809	262.7132	5.7641	225.5014	16.4414	581.4723	2.0128	555.1168
	SB5	215.4766	1558.047	205.02	1428.302	−8.1868	181.1595	−12.5455	193.4318
	SB6	1125.727	6887.929	968.5325	5124.709				

Table 12
Statistical parameters (mean (M) and standard deviation (STD)) calculated for LE feature obtained from EMD and WT methods.

		WT - 5 level				EMD - IMF - 5			
		HT		HC		HT		HC	
		M	STD	M	STD	M	STD	M	STD
LE	SB1	−7070.99	2415.091	−6793.74	2799.963	−8971.64	1692.448	−8413.95	2151.292
	SB2	−16645.8	1474.562	−16860.5	1663.159	−8108.93	2112.1	−7538.75	2433.392
	SB3	−12889.3	1122.569	−13238.7	1532.718	−8029.15	1999.762	−7916.51	2432.219
	SB4	−9691.83	1379.299	−9806.66	1674.689	−9963.09	2166.934	−9953.8	2588.704
	SB5	−8873.26	1646.877	−8286.6	2191.616	−11690.6	2508.929	−11491.3	2918.19
	SB6	−8254.43	2162.676	−7782.69	2633.485				

Table 13
Comparison with literature.

S.No.	Author/Year	Used Signal	Used Feature	Technique	Size	Type of Database	Performance %
1	Y.Song et al. [8]	HRV	Nonlinear	EEMD	18	Private	Acc = 74.35
2	Liu et al. [5]	HRV	HRV, linear, nonlinear, time, frequency domain	CAR	128	Public	Acc = 84.45
3	Proposed	BCG	Nonlinear	WT, EMD	128	Public	Acc = 89(WT), 78.78(EMD)

EEMD = Empirical Ensemble Mode Decomposition, CAR = Classification Association Rule, Acc = Accuracy.

accurate and robust as we employed a 10-fold cross-validation method. Subsequently, there is no possibility of an overfitting problem.

The limitation of the proposed work are give below:

The drawback of the smart mattress-based BCG data recording is that it limits the activity of the subjects and hence may not be able to record high-quality BCG signals. Additionally, the recording of BCG signals during daytime activities of subjects is not possible as it is not possible to use a smart mattress-based system. To obtain the high-quality BCG signal Smartwatches, wearable gadgets, and smart chairs are ideal methods to record the BCG signal in the daytime also.

The BCG-based systems yield the best performance. The latter may be more useful as it requires a smaller bandwidth. Using cutting-edge machine learning, deep learning methodologies, the performance of BCG-based systems, can be improved [37–39].

6. Conclusion

An automated system for the detection of HT is proposed using WT and nonlinear features. We have obtained the detection accuracy of 89% using EGB classifier. The main drawback of this system is that, we have used a small database to develop this prototype. In future, we plan to use bigger diverse database to extend this work and also use deep learning techniques. Also, other nonlinear features like higher spectra and entropies can be employed to boost the classification performance.

Declaration of competing interest

The authors declare that they have no known competing financial interests or personal relationships that could have appeared to influence the work reported in this paper.

References

[1] Unger T, Borghi C, Charchar F, Khan N, Poulter N, Dorairaj P, Ramirez A, Schlaich M, Stergiou G, Tomaszewski M, Wainford R, Williams B, Schutte A. International society of hypertension global hypertension practice guidelines. Hypertension 2020;75. http://dx.doi.org/10.1161/HYPERTENSIONAHA.120.15026.

[2] Rajput JS, Sharma M, Acharya UR. Hypertension diagnosis index for discrimination of high-risk hypertension ecg signals using optimal orthogonal wavelet filter bank. Int J Environ Res Public Health; 16 (21). URL https://www.mdpi.com/1660-4601/16/21/4068.

[3] Soh D, Ng E, Vicnesh J, Oh SL, Tan RS, Acharya UR. A computational intelligence tool for the detection of hypertension using empirical mode decomposition. Comput Biol Med 2020;118:103630. http://dx.doi.org/10.1016/j.compbiomed.2020.103630.

[4] Rajput JS, Sharma M, Tan RS, Acharya UR. Automated detection of severity of hypertension ecg signals using an optimal bi-orthogonal wavelet filter bank. Comput Biol Med 2020;103924. http://dx.doi.org/10.1016/j.compbiomed.2020.103924, URL http://www.sciencedirect.com/science/article/pii/S001048252030264X.

[5] Liu F, Zhou X, Wang Z, Cao J, Wang H, Zhang Y. Unobtrusive mattress-based identification of hypertension by integrating classification and association rule mining. Sensors 2019;19:1489. http://dx.doi.org/10.3390/s19071489.

[6] Sharma M, Rajput JS, Tan RS, Acharya UR. Automated detection of hypertension using physiological signals: A review. Int J Environ Res Public Health; 18 (11). http://dx.doi.org/10.3390/ijerph18115838. URL https://www.mdpi.com/1660-4601/18/11/5838.

[7] Sadek I, Biswas J, Abdulrazak B. Ballistocardiogram signal processing: a review. Health Inform Sci Syst; 7. http://dx.doi.org/10.1007/s13755-019-0071-7.

[8] Song Y, Ni H, Zhou X, Zhao W, Wang T. Extracting features for cardiovascular disease classification based on ballistocardiography. 2015, p. 1230–5. http://dx.doi.org/10.1109/UIC-ATC-ScalCom-CBDCom-IoP.2015.223.

[9] Chen Z, Yang X, Teo JT, Ng S. Noninvasive monitoring of blood pressure using optical ballistocardiography and photoplethysmograph approaches. In: Conference proceedings :... Annual international conference of the ieee engineering in medicine and biology society. vol. 2013, IEEE Engineering in Medicine and Biology Society. Conference; 2013, p. 2425–8. http://dx.doi.org/10.1109/EMBC.2013.6610029.

[10] Lee K, Roh J, Cho D, Hyeong J, Kim S. A chair-based unconstrained/nonintrusive cuffless blood pressure monitoring system using a two-channel ballistocardiogram. Sensors 2019;19:595. http://dx.doi.org/10.3390/s19030595.

[11] Seok W, Lee K, Cho D, Roh J, Kim S. Blood pressure monitoring system using a two-channel ballistocardiogram and convolutional neural networks. Sensors 2021;21:2303. http://dx.doi.org/10.3390/s21072303.

[12] Inan O, Migeotte P-F, Park K, Etemadi M, Tavakolian K, Casanella R, Zanetti J, Tank J, Funtova I, Prisk K, Di Rienzo M. Ballistocardiography and seismocardiography: A review of recent advances. IEEE J Biomed Health Inform; 19. http://dx.doi.org/10.1109/JBHI.2014.2361732.

[13] Jain A, Nandakumar K, Ross A. Score normalization in multimodal biometric system. Pattern Recognit 2005;38:2270–85. http://dx.doi.org/10.1016/j.patcog.2005.01.012.

[14] Sharma M, Kolte R, Patwardhan P, Gadre V. Time-frequency localization optimized biorthogonal wavelets. In: Int. conf. on signal process. and comm., vol. 2010; 2010. p. 1–5.

[15] Stasiakiewicz P, Dobrowolski AP, Targowski T. Automatic classification of normal and sick patients with crackles using wavelet packet decomposition and support vector machine. Biomed Signal Process Control 2021;67:102521. http://dx.doi.org/10.1016/j.bspc.2021.102521, URL https://www.sciencedirect.com/science/article/pii/S174680942100118X.

[16] Sharma M, Acharya UR. Analysis of knee-joint vibroarthographic signals using bandwidth-duration localized three-channel filter bank. Comput Electr Eng 2018;72:191–202. http://dx.doi.org/10.1016/j.compeleceng.2018.08.019, URL http://www.sciencedirect.com/science/article/pii/S0045790618311017.

[17] Sharma M, Gadre VM, Porwal S. An eigenfilter-based approach to the design of time-frequency localization optimized two-channel linear phase biorthogonal filter banks. Circ Syst Signal Process 2015;34(3):931–59.

[18] Sharma M, Acharya UR. Automated detection of schizophrenia using optimal wavelet-based l_1 norm features extracted from single-channel eeg. Cogn Neurodyn 2021;1–14–w. http://dx.doi.org/10.1007/s11571-020-09655.

[19] Sharma M, Tiwari J, Patel V, Acharya UR. Automated identification of sleep disorder types using triplet half-band filter and ensemble machine learning techniques with eeg signals. Electronics 2021;10:1531. http://dx.doi.org/10.3390/electronics10131531.

[20] Mookiah MRK, Acharya UR, Fujita H, Koh JEW, Tan JH, Chua K, Bhandary S, Noronha K, Laude A, Tong L. Automated detection of age-related macular degeneration using empirical mode decomposition. Knowl-Based Syst 2015;89:654–68. http://dx.doi.org/10.1016/j.knosys.2015.09.012.

[21] Bhati D, Sharma M, Pachori RB, Nair SS, Gadre VM. Design of time–frequency optimal three-band wavelet filter banks with unit sobolev regularity using frequency domain sampling. Circuits Systems Signal Process 2016;35(12):4501–31.

[22] Sharma M, Tan R-S, Acharya UR. Automated heartbeat classification and detection of arrhythmia using optimal orthogonal wavelet filters. Inform Med Unlocked 2019;100221. http://dx.doi.org/10.1016/j.imu.2019.100221, URL http://www.sciencedirect.com/science/article/pii/S2352914819301091.

[23] Sharma M, Tan RS, Acharya UR. A novel automated diagnostic system for classification of myocardial infarction ecg signals using an optimal biorthogonal filter bank. Comput Biol Med. http://dx.doi.org/10.1016/j.compbiomed.2018.07.005. URL http://www.sciencedirect.com/science/article/pii/S0010482518301884.

[24] Sharma M, Acharya UR. A new method to identify coronary artery disease with ecg signals and time-frequency concentrated antisymmetric biorthogonal wavelet filter bank. Pattern Recognit Lett 2019;125:235–40. http://dx.doi.org/10.1016/j.patrec.2019.04.014, URL http://www.sciencedirect.com/science/article/pii/S0167865519301217.

[25] Sharma M, Raval M, Acharya UR. A new approach to identify obstructive sleep apnea using an optimal orthogonal wavelet filter bank with ecg signals. Inform Med Unlocked 2019;100170. http://dx.doi.org/10.1016/j.imu.2019.100170, URL http://www.sciencedirect.com/science/article/pii/S235291481930022X.

[26] Sharma M, Bhurane AA, Acharya UR. MMSFL-OWFB: A novel class of orthogonal wavelet filters for epileptic seizure detection. Knowl-Based Syst 2018;160:265–77. http://dx.doi.org/10.1016/j.knosys.2018.07.019.

[27] Sharma M, Sharma P, Pachori RB, Acharya UR. Dual-tree complex wavelet transform-based features for automated alcoholism identification. Int J Fuzzy Syst 2018;20(5):1297–308. http://dx.doi.org/10.1007/s40815-018-0455-x, URL https://link.springer.com/article/10.1007/s40815-018-0455-x.

[28] Sharma M, Patel V, Acharya UR. Automated identification of insomnia using optimal bi-orthogonal wavelet transform technique with single-channel eeg signals. Knowl-Based Syst 2021;107078. http://dx.doi.org/10.1016/j.knosys.2021.107078, URL https://www.sciencedirect.com/science/article/pii/S0950705121003415.

[29] Sharma M, Tiwari J, Acharya UR. Automatic sleep-stage scoring in healthy and sleep disorder patients using optimal wavelet filter bank technique with eeg signals. Int J Environ Res Public Health; 18 (6). http://dx.doi.org/10.3390/ijerph18063087. URL https://www.mdpi.com/1660-4601/18/6/3087.

[30] Sharma M, Dhiman HS, Acharya UR. Automatic identification of insomnia using optimal antisymmetric biorthogonal wavelet filter bank with ecg signals. Comput Biol Med 2021;104246. http://dx.doi.org/10.1016/j.compbiomed.2021.104246, URL https://www.sciencedirect.com/science/article/pii/S0010482521000408.

[31] M, Kumbhani D, Yadav A, Acharya UR. Automated sleep apnea detection using optimal duration-frequency concentrated wavelet-based features of pulse oximetry signals. Appl Intel. http://dx.doi.org/10.1007/s10489-021-02422-2.

[32] Zala J, Sharma M, Bhalerao R. Tunable q - wavelet transform based features for automated screening of knee-joint vibroarthrographic signals. In: 2018 International conference on signal processing and integrated networks; 2018.

[33] Shah S, Sharma M, Deb D, Pachori RB. An automated alcoholism detection using orthogonal wavelet filter bank. In: 2019 international conference on machine intelligence and signal analysis advances in intelligent systems and computing. vol. 748, Singapore: Springer; 2019, p. 473–83. http://dx.doi.org/10.1007/978-981-13-0923-6_41.

[34] Timčenko V, Gajin S. Ensemble classifiers for supervised anomaly based network intrusion detection. In: 2017 13th IEEE international conference on intelligent computer communication and processing. IEEE; 2017, p. 13–9.

[35] Oh D-Y, Gray JB. Ga-ensemble: a genetic algorithm for robust ensembles. Comput Statist 2013;28(5):2333–47.

[36] Ali S, Majid A, Javed SG, Sattar M. Can-csc-gbe: Developing cost-sensitive classifier with gentleboost ensemble for breast cancer classification using protein amino acids and imbalanced data. Comput Biol Med 2016;73:38–46.

[37] Oh SL, Vicnesh J, Tan RS, Ciaccio E, Yamakawa T, Tanabe M, Kobayashi M, Faust O, Acharya UR. Comprehensive electrocardiographic diagnosis based on deep learning. Artif Intell Med; 103. http://dx.doi.org/10.1016/j.artmed.2019.101789.

[38] yıldırım z, Baloglu U, Tan RS, Ciaccio E, Acharya UR. A new approach for arrhythmia classification using deep coded features and lstm networks. Comput Methods Programs Biomed 2019;176:121–33. http://dx.doi.org/10.1016/j.cmpb.2019.05.004.

[39] yıldırım z, Talo M, Ciaccio E, Tan RS, Acharya UR. Accurate deep neural network model to detect cardiac arrhythmia on more than 10, 000 individual subject ecg records. Comput Methods Programs Biomed; 197. http://dx.doi.org/10.1016/j.cmpb.2020.105740.